Review of Scientific Instruments

Additively manufactured electrodes for plasma and power-flow studies in high-power transmission lines on the 1-MA MAIZE facility

Cite as: Rev. Sci. Instrum. **92**, 053550 (2021); https://doi.org/10.1063/5.0043856
Submitted: 11 January 2021 . Accepted: 28 April 2021 . Published Online: 25 May 2021

T. J. Smith, P. C. Campbell, G. V. Dowhan, N. M. Jordan, M. D. Johnston, M. E. Cuneo, G. R. Laity, and R. D. McBride

AIP Publishing

Review of Scientific Instruments ARTICLE scitation.org/journal/rsi

Additively manufactured electrodes for plasma and power-flow studies in high-power transmission lines on the 1-MA MAIZE facility

Cite as: Rev. Sci. Instrum. 92, 053550 (2021); doi: 10.1063/5.0043856
Submitted: 11 January 2021 • Accepted: 28 April 2021 •
Published Online: 25 May 2021

T. J. Smith,[1,a] P. C. Campbell,[1] G. V. Dowhan,[2] N. M. Jordan,[1] M. D. Johnston,[3] M. E. Cuneo,[3] G. R. Laity,[3] and R. D. McBride[1,2]

AFFILIATIONS

[1] Nuclear Engineering and Radiological Sciences, University of Michigan, Ann Arbor, Michigan 48109, USA
[2] Applied Physics Program, University of Michigan, Ann Arbor, Michigan 48109, USA
[3] Sandia National Laboratories, Albuquerque, New Mexico 87185, USA

Note: Paper published as part of the Special Topic on Proceedings of the 23rd Topical Conference on High-Temperature Plasma Diagnostics.
[a] **Author to whom correspondence should be addressed:** smtrevor@umich.edu

ABSTRACT

Power-flow studies on the 30-MA, 100-ns Z facility at Sandia National Laboratories have shown that plasmas in the facility's magnetically insulated transmission lines (MITLs) and double post-hole convolute can result in a loss of current delivered to the load. To study power-flow physics on the 1-MA, 100-ns MAIZE facility at the University of Michigan, planar MITL loads and planar post-hole convolute loads have been developed that extend into the lines of sight for various imaging diagnostics on MAIZE. These loads use 3D-printed dielectric support structures lined with thin foils of either aluminum or stainless steel. The metal foils serve as the current-carrying power-flow surfaces, which generate plasma during the current pulse. The foil thickness (50 μm) and widths (11.5–16 mm) are selected to ensure a sufficient linear current density (0.5–0.7 MA/cm) for plasma formation. Laser backlighting (532 nm) and visible-light self-emission imaging capture the overall plasma evolution in the anode–cathode gaps, including the gap closure velocities (1–4 cm/μs).

I. INTRODUCTION

The 30-MA, 100-ns Z facility at Sandia National Laboratories uses magnetically insulated transmission lines (MITLs)[1] and a double post-hole convolute[2] to efficiently deliver power to high-energy-density physics experiments.[3] Due to the intense ohmic heating of the MITL electrodes, neutral surface layer contaminants (water, hydrogen, hydrocarbons, etc.) desorb and ionize to form plasmas in the anode–cathode (AK) gap. With a sufficient magnetic field strength in the AK gap, this plasma is nominally held close to its originating electrode. However, in some cases, electrode plasmas can bridge the AK gap, causing power loss upstream of the load/target.[4–10]

These power-flow plasmas on the Z facility are generated from extremely high linear current densities heating the electrode surfaces to well over 400 °C.[8,11] Note that these are essentially surface currents, as the electrical skin depth of a current pulse with a 100-ns rise time, in a common electrode material such as stainless steel, is ~100 μm, which is much less than the thickness of a typical electrode (~1 cm).

On the Z facility, B-dot probes and fiber-based visible spectroscopy probes are placed in the MITL and post-hole convolute regions to characterize the current delivery and the plasma densities and temperatures.[2] However, these diagnostics have very limited viewing angles, so they make very local measurements.

To broadly image plasmas flowing through MITL and post-hole convolute structures, planar geometries can be used to enable side-on viewing (rather than closed axisymmetric geometries with no side-on access). Such geometries have been explored previously in scaled experiments on smaller (~1 MA) university facilities—e.g., the 0.5–1-MA, 100–250-ns MAIZE facility at the University of Michigan[12] and the 1-MA, 100–200-ns COBRA facility at Cornell University.[13] An additional challenge for scaled experiments on university facilities is that the linear current densities are

typically not high enough to source detectable amounts of plasma from the surfaces of thick metal electrodes. To source observable amounts of plasma, additional steps must be taken. For example, in Ref. 13, UV light from an exploding wire strung across the AK gap is used to photoionize neutral particles desorbed from the electrode surfaces.

At the University of Michigan, a new approach has been taken for sourcing plasma from custom-shaped electrode surfaces at the 0.5–1 MA level. This approach uses 3D-printed dielectric support structures that are lined with thin aluminum foils. During the current pulse, these thin foils serve as the current-carrying power-flow surfaces, maximizing the heat delivery to surface contaminants and thus increasing the plasma generation to detectable levels. These plasmas are not driven to the extreme conditions found in the MITLs on the Z facility; nonetheless, this platform does leverage university-scaled driver currents on similar timescales for addressing power-flow relevant physics issues—e.g., the dynamics of low-density plasma in complex MITL and post-hole convolute structures. The ultimate goal is to validate computational models that can be scaled to the conditions found on the Z facility and to help motivate future experiments on the Z facility. Additionally, due to the versatility of 3D printing, this approach enables plasma and power-flow studies in complex MITL and post-hole convolute geometries. The remainder of this paper describes the development and demonstration of this approach. Examples are provided for both planar MITL and planar post-hole convolute structures.

II. EXPERIMENTAL DESIGN AND DEMONSTRATION

An example of a 3D-printed planar MITL load and its experimental data are presented in Fig. 1. The loads were tested on the MAIZE linear transformer driver (LTD) facility,[14] which was charged to ±70 kV to deliver ~800 kA in 150–200 ns under high vacuum conditions (~10^{-5} Torr). The load is placed on top of the output of MAIZE's conical power feed[15] to enable either side-on laser shadowgraphy or self-emission imaging of the plasma expansion into the AK gap of the MITL load (shadowgraphy is presented in Fig. 1). The load current was measured using a 20-turn Rogowski coil embedded in the MAIZE anode at a radius of 11 cm.

The primary constraints for designing these planar MITL loads were the size of MAIZE's output AK gap (4.8 mm), the output diameter of MAIZE's circular cathode stalk (16 mm), and the height of the imaging field of view, measured from the top of the cathode stalk to the top of the vacuum chamber windows (70 mm). The initial MITL load design (presented in Fig. 1) had an AK gap of 13 mm, a width of 16 mm, and a height of 45 mm. After initial tests, the foil plasmas were not closing the gaps on the same timescale as the current pulse (see Fig. 2), so a smaller target was designed with a gap size, width, and height of 4.8, 11.5, and 25 mm, respectively (see Fig. 3). The smaller target allowed for much of the experiment to be observable, full gap closure within the timescale of the current pulse (see Fig. 3), and an increase in linear current density from 0.5 to 0.7 MA/cm. While more current density is desirable, we also want to maintain a wide enough load to prevent edge effects from perturbing the plasma formation and evolution.

The dielectric support structures were additively manufactured using a Formlabs Form-2 Stereolithography (SLA) printer. This enabled rapid fabrication and prototyping of complex geometries with a printing precision of ±50 μm. A batch of 15 planar MITL structures can be printed in as little as 15 hours. The material used for the first round of experiments was the Formlabs "Durable Resin," which is similar to polypropylene.[16] The Durable Resin was chosen for its ability to withstand the high experimental pressures while also being somewhat flexible and having good dielectric hold off properties. In the initial tests with the larger target designs, the support structures often survived the experiments (though the foils were vaporized). However, when switching to the smaller target dimensions, the increased magnetic and thermal pressures destroyed the support structures each time, so we switched to the Formlabs "Tough Resin," which is able to withstand higher pressures, but with less elasticity.[16]

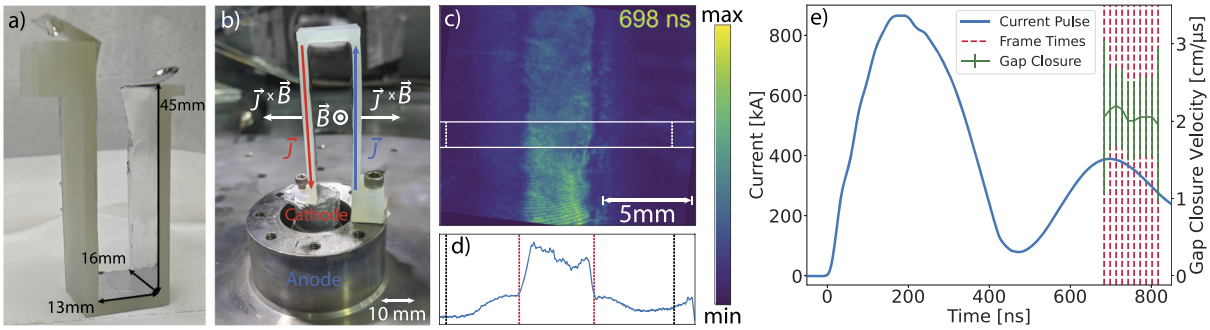

FIG. 1. (a) Photograph of a planar MITL load, where the 3D-printed dielectric support structure has been lined with a thin metal foil. (b) Photograph of the load shown in (a) installed in MAIZE. The directions of the current density $\vec{j}$, the magnetic field $\vec{B}$, and the force density $\vec{j} \times \vec{B}$ are indicated. Labeled in blue is the MAIZE anode (outer cylindrical electrode) and in red is the MAIZE cathode (inner cylindrical electrode). (c) An example laser shadowgraph taken during MAIZE experiment 1703, showing very late-time plasma expansion into the AK gap. The vertical dashed white lines indicate the initial position of the foil, while the overlaid horizontal white lines indicate the region used to generate the 1D lineout presented in (d). In (d), the plasma location is indicated by the vertical dashed red lines, while the initial position of the foil is indicated by the vertical dashed black lines. The full width of the image (c) and lineout (d) is 14.5 mm. (e) Measured load current and gap closure velocities determined from the shadowgraphs collected on shot 1703; the shadowgraph times are indicated by the vertical dashed red lines (only 10 of the 12 shadowgraphs collected in this experiment were usable).

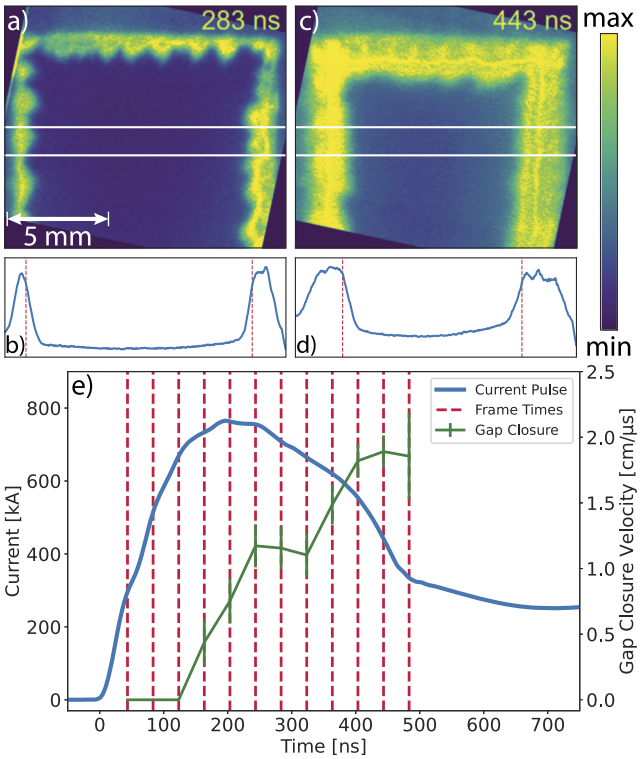

FIG. 2. (a) and (c) Visible-light self-emission images from shot 1706, which used the larger (13 mm × 16 mm × 45 mm) planar MITL load. The white horizontal lines indicate the regions used for the 1D lineouts presented in (b) and (d). In (b) and (d), the plasma location is indicated by the vertical dashed red lines. (e) The current profile and gap closure velocities; the vertical dashed red lines indicate the image times collected. The full width of each image (a) and (c) and lineout (b) and (d) is 14 mm.

Note that the support structures can also be made thicker to accommodate higher pressures and higher electric field strengths. This can be useful for mitigating explosive debris, especially when sensitive diagnostics are placed near the load or within the support structure itself. Additionally, increasing the printed structure's thickness-to-height aspect ratio reduces warping due to the thermomechanical stresses that are present during the printing and curing stages. Warping and AK gap compression during vacuum pump down can affect the uniformity of the load's AK gap spacing, but a tolerance of a few degrees off parallel was deemed acceptable.

Referring to Figs. 1(a) and 1(b), each foil is roughly cut to the length and width of its support structure. A thin layer of strong epoxy is applied to the inner surface of the support structure and spread to form an almost uniform coating. The foil is then laid into the gap, stretched into the top corners of the target using two thin straight edges, and gently pressed against the sides of the structure, moving slowly downward from the top of the target to the base of the target (the base being where the target attaches to the MAIZE anode and cathode via two screws). The rest of the foil is draped over the bottom surface of the structure so that it makes good electrical contact with the MAIZE anode and cathode. Any excess foil extending

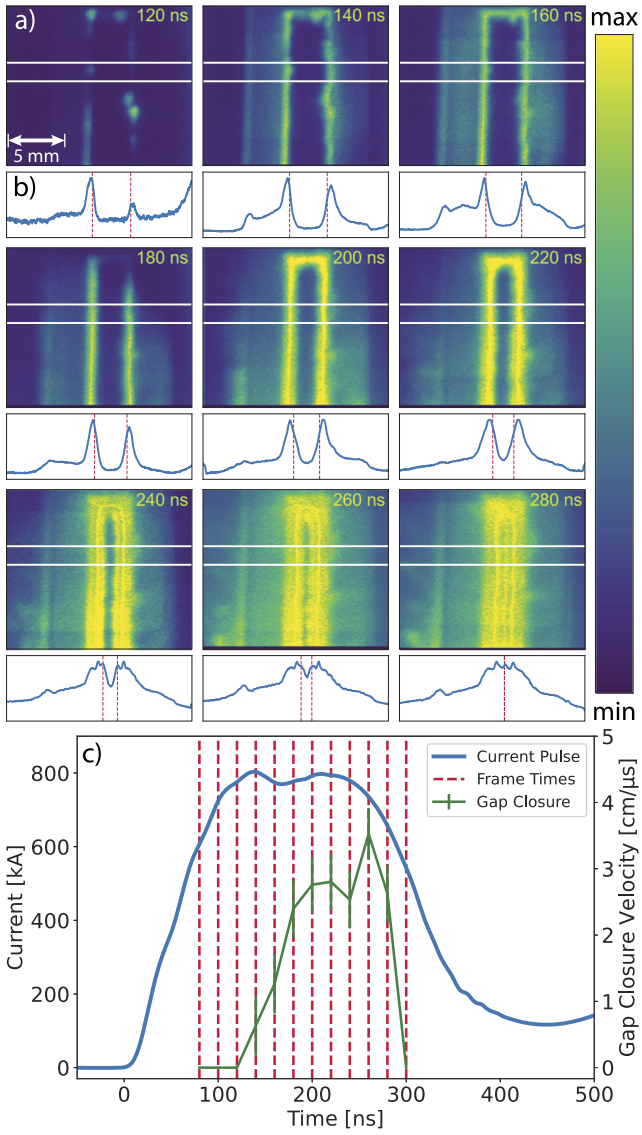

FIG. 3. (a) Visible-light self-emission images from shot 1719, which used the smaller (4.8 mm × 11.5 mm × 25 mm) planar MITL load. Here, plasma can be seen closing the 4.8-mm AK gap. The white horizontal lines in each image indicate the region used for the 1D lineout presented immediately below each image, labeled as (b). In each 1D lineout, the plasma location is indicated by the vertical dashed red lines. (c) The current profile and gap closure velocities; the vertical dashed red lines indicate the image times collected. The full width of each image (a) and lineout (b) is 18 mm.

beyond the width of the support structure is shaved off using a razor blade. The target is then left undisturbed for the epoxy to cure. A special cathode attachment was made to screw the target to the MAIZE cathode, and one of the eight tapped holes in MAIZE's anode was used for the anode attachment.

The foil used in these experiments was 50-μm-thick aluminum (±15%),[17] which is thinner than the electrical skin depth (65–75 μm) of a 150–200-ns current pulse. Thus, the current was distributed

relatively uniformly in the foil during the initial resistive heating stage. As the foil heats, it begins to generate plasma that expands into the anode–cathode gap [see Fig. 1(c)]. Despite the foils being completely vaporized on every shot, the support structures showed no signs of degradation from plasma heating during the current pulse. This suggests that the current was largely confined to the foil material, as intended. However, there were also no signs of epoxy left on the support structures; thus, ionized epoxy material might have carried some of the current.

The $\vec{j} \times \vec{B}$ force density (or magnetic pressure) resists the plasma expansion into the AK gap [see Fig. 1(b)]. However, at late times, when the current pulse has decayed and significant thermal energy has been deposited into the expanding plasma, rapid gap closure (~2 cm/μs) ensues [see Fig. 1(e)]. Note that the magnetic pressure attempts to drive the foil plasma outward (i.e., this is an exploding geometry[18]), but the mass and strength of the dielectric support structure prevent outward expansion, acting as a confining rigid MITL. Thus, the plasma dynamics become a competition between the thermal pressure driving the plasma into the AK gap and the magnetic pressure resisting this inward expansion.

For imaging the plasmas, an Invisible Vision Ultra UHSi intensified charge-coupled device (ICCD) enabled either 12-frame laser shadowgraphy or 12-frame visible-light self-emission imaging with 1000 × 860 pixel resolution.[15] The laser used for shadowgraphy is a frequency-doubled Nd:YAG source (532 nm) that supplies a single 125-mJ, 2-ns pulse. An optical cavity is used to split the single laser pulse into a semi-infinite pulse train with 15-ns intervals, where the first 12 pulses (each with $\lesssim$0.25% of the initial pulse energy) are synchronized to the 15-ns exposures of the 12-frame ICCD camera.[15] The time resolution of the shadowgraphs is determined by the laser pulse width (2 ns).

The visible-light self-emission imaging system uses the same receiving optics and 12-frame ICCD camera as the laser shadowgraphy system, but it images the light emitted from the ablating foil plasma. The camera exposure time can be as low as 5 ns, but in Figs. 2 and 3, 15-ns exposures with 40 and 20 ns between frames, respectively, were used to ensure adequate light collection throughout the main current pulse.

Using the time between frames and the position of the foil plasma in each frame (from 1D lineouts), the gap closure velocity has been calculated and is plotted with the current traces in Figs. 1–3 (note that with the convention used in this paper, the AK gap closure velocity is approximately twice the plasma expansion velocity away from a given electrode surface). The horizontal 1D lineouts are formed by averaging over 100 consecutive pixel rows in the vertical direction (1.45 mm). The areas selected for the 1D lineouts are the areas between the white horizontal lines in Figs. 1–3. The lineouts are used to identify (by eye) the location of the expanding plasma. These locations are indicated by the vertical dashed red lines in each of the lineouts plotted in Figs. 1–3. For the laser shadowgraphy lineouts [e.g., Fig. 1(c)], the left and right plasma locations are defined by the abrupt transitions at the outer edges of the central maximum-intensity region. For the lineouts from the visible-light self-emission images (e.g., Figs. 2 and 3), the left and right plasma locations are defined by the inflection points immediately surrounding the central minimum-intensity region. Note that in the final frame of Fig. 3 (280 ns), complete gap closure has occurred, and bright plasma has accumulated at the center of the AK gap. Thus, there is no central minimum in the 1D lineout of the 280-ns frame; instead, there is a local maximum.

The error bars for the gap closure velocities in Figs. 1–3 were determined from the 150-μm (ten-pixel) spatial resolution and 2-ns timing resolution of the imaging data. Note that the 150-μm spatial resolution includes 50 μm of motional blur. The uncertainties were added in quadrature while accounting for the linear correlation between interframe times and gap-width variables. Slight image rotation corrections were also applied while maintaining the original 1000 × 860 pixel resolution. All image intensities displayed for a given shot have been normalized to the same linear scale (in arbitrary units) and make use of Python's MatPlotLib "viridis" colormap, which has been designed to uniformly display gradual changes in intensity (i.e., there are no color jumps that would preferentially accentuate some features over others).[19,20] The lineout intensities are also on a linear scale, but they are normalized to the peak value in each lineout. The images have a 1:1 aspect ratio for vertical and horizontal spatial scales, and all spatial scales are linear.

As shown in Fig. 1 (shot 1703), laser shadowgraphy was used to study very late-time plasma dynamics in the AK gap of the larger of the two planar MITL loads tested. As this was the first experiment conducted after rebuilding MAIZE with upgraded L3Harris spark-gap switches (model 50264), there was uncertainty in the timing of the imaging system relative to the current pulse. As a result, the camera captured the gap closing roughly 500 to 600 ns after peak current.

In Fig. 2 (shot 1706), the larger of the two target designs was again used, but in this case, visible-light self-emission imaging captured the plasma dynamics during the main current pulse. Here, the foil starts to heat and generate plasma, which expands into the gap at up to 1.8 cm/μs. In the earlier image, a periodic structure appears in the plasma. The spatial period is not completely uniform, but it is in the range of 1–2 mm. In the later image, the periodic structure smooths out as the plasma expands into the gap.

In Fig. 3 (shot 1719), self-emission imaging was again used to capture the plasma dynamics during the main current pulse, but in this case, the smaller target design was used. The peak current of 800 kA corresponds to a linear current density of 0.70 MA/cm. Use of this target resulted in higher gap closure velocities (2.5–3.5 cm/μs). Additionally, because of the decreased AK gap, the time needed for the plasma to close the gap was decreased.

Note that in both Figs. 2 and 3 (and throughout the ten-shot series, which included six shots with the larger target and four shots with the smaller target), a step increase in the gap closure velocity appears to occur as the current (and thus magnetic pressure) begins to fall (although in Fig. 3, this increase is only briefly observed before complete gap closure occurs).

III. CONCLUSIONS AND FUTURE WORK

The approach demonstrated in this paper enables the study of power-flow plasmas at the 0.5–1-MA level in diagnostically accessible geometries. The gap closure velocities measured were in the range of 1–4 cm/μs (throughout the ten-shot series), which is consistent with that found in the literature.[4–7,9,10] The planar MITL load demonstrated in this paper is particularly relevant to the stripline loads used to study dynamic material properties on the Z facility at Sandia, where plasma filling the AK gap can affect the magnetic drive

pressure applied to the material sample (e.g., see Figs. 1 and 2 in Ref. 21).

In future experiments, spectroscopy techniques will be applied to determine the plasma's temperature, density, and constituents (including contaminant populations such as hydrogen and carbon). Furthermore, Zeeman spectroscopy and Faraday rotation imaging will be applied to measure the magnetic field in the AK gaps and determine the degree of magnetic insulation. Also, from Figs. 2 and 3, it is important to understand how the observed periodic structures are formed. Using a slightly off-angle line-of-sight will allow us to determine if the periodic structures span the width of the foil or if they are located only at the edges of the foil.

As an example of where this approach can be taken in the future, in Fig. 4, we present a planar post-hole convolute design that has now been fabricated and is in preliminary testing on MAIZE. This design uses two post-hole convolutes. An outer post-hole convolute splits MAIZE's output power feed into two parallel planar MITL levels. These two levels are then recombined into a single planar MITL via a second (inner) post-hole convolute. The planar geometry and small size of the 3D-printed design enables side-on imaging with a field of view that includes the upper and lower MITLs, the inner post-hole convolute, and the load region [see Fig. 4(a)]. This allows us to investigate how plasma flows through a post-hole convolute and up into a load region. These flows can then be compared with simulations similar to those presented in Ref. 8. The different anode and cathode levels can be printed in a dielectric material and lined with foil such as the planar MITL targets described in Figs. 1–3. In Fig. 4, the dielectric pieces are lighter colored (i.e., lighter red for the cathode pieces and lighter blue for the anode pieces). The rest of the pieces can be 3D printed or machined in metal to provide mechanical stability and reusability; these thick solid-metal pieces are expected to source relatively little plasma. Thus, we can control which surfaces source plasma by controlling which sections are made from foil-lined dielectric vs which sections are made from thick solid metal. Note that in some complex assemblies, it may be difficult to line a dielectric piece with foil. In these cases, various metal deposition methods can be used.

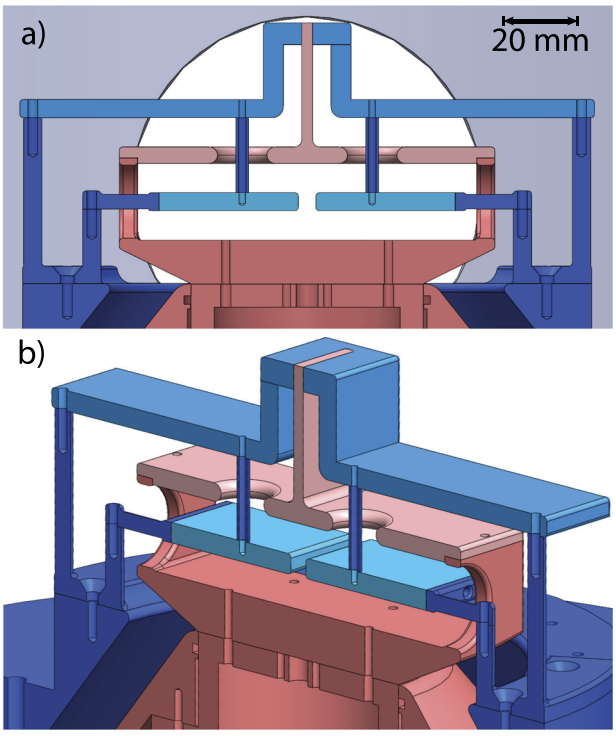

FIG. 4. (a) Side-on drawing of a 3D-printed post-hole convolute ("print-a-lute"). (b) Isometric view of the print-a-lute. In (a) and (b), the foil-lined dielectric pieces are lighter colored (i.e., lighter red for the cathode pieces and lighter blue for the anode pieces). The darker colored pieces are solid metal.

ACKNOWLEDGMENTS

This work was supported by Sandia National Laboratories through the Campus Executives and LDRD Programs, Project No. 20-9240. Additional support was provided by DOE Cooperative Grant Agreement No. DE-NA0003764. Sandia National Laboratories is a multi-mission laboratory managed and operated by the National Technology and Engineering Solutions of Sandia, LLC, a wholly owned subsidiary of Honeywell International, Inc., for the U.S. DOE-NNSA under Contract No. DE-NA0003525. This paper describes objective technical results and analysis. Any subjective views or opinions that might be expressed in the paper do not necessarily represent the views of the U.S. Department of Energy or the U.S. Government.

DATA AVAILABILITY

The data that support the findings of this study are available from the corresponding author upon reasonable request.

REFERENCES

[1]W. A. Stygar *et al.*, Phys. Rev. Spec. Top.-Accel. Beams **12**, 120401 (2009).
[2]M. R. Gomez *et al.*, Phys. Rev. Accel. Beams **20**, 010401 (2017).
[3]D. B. Sinars *et al.*, Phys. Plasmas **27**, 070501 (2020).
[4]R. W. Stinnett *et al.*, IEEE Trans. Electr. Insul. **EI-20**, 807 (1985).
[5]V. V. Ivanov, P. J. Laca, B. S. Bauer, R. Presura, V. I. Sotnikov, A. L. Astanovitskiy, B. Le Galloudec, J. Glassman, and R. A. Wirtz, IEEE Trans. Plasma Sci. **32**, 1843 (2004).
[6]Y. L. Bakshaev *et al.*, Plasma Phys. Rep. **33**, 259 (2007).
[7]S. S. Anan'ev *et al.*, Plasma Phys. Rep. **34**, 574 (2008).
[8]D. V. Rose, E. A. Madrid, D. R. Welch, R. E. Clark, C. B. Mostrom, W. A. Stygar, and M. E. Cuneo, Phys. Rev. Spec. Top.-Accel. Beams **18**, 030402 (2015).
[9]S. A. Slutz *et al.*, Phys. Plasmas **25**, 112706 (2018).
[10]R. B. Baksht, A. S. Zhigalin, A. G. Rousskikh, and V. I. Oreshkin, Phys. Plasmas **27**, 043510 (2020).
[11]A. E. Blaugrund, G. Cooperstein, and S. A. Goldstein, Phys. Fluids **20**, 1185 (1977).
[12]M. R. Gomez, Ph.D. thesis, University of Michigan, 2011
[13]J. Greenly, Paper GP17 11, Bull. Am. Phys. Soc. **65**, 125 (2020), see https://meetings.aps.org/Meeting/DPP20/Session/GP17.11.
[14]R. M. Gilgenbach *et al.*, AIP Conf. Proc. **1088**, 259 (2009).
[15]P. C. Campbell *et al.*, IEEE Trans. Plasma Sci. **46**, 3973 (2018).
[16]See https://formlabs.com/ for 3D resin material properties.
[17]See http://www.goodfellow.com/ for metal foil properties.
[18]R. D. McBride *et al.*, IEEE Trans. Plasma Sci. **46**, 3928 (2018).
[19]J. D. Hunter, Comput. Sci. Eng. **9**, 90 (2007).
[20]See https://bids.github.io/colormap/ for an overview on the "viridis" colormap.
[21]A. Porwitzky, B. T. Hutsel, C. T. Seagle, T. Ao, S. Grant, A. Bernstein, J.-F. Lin, and T. Ditmire, Phys. Rev. Accel. Beams **22**, 090401 (2019).